e-ISSN: 2149-4584

Erzincan University Journal of Science and Technology

EJSAT 2025, 18 (3) 842-857

Research Article

Lepton Flavor Violating Tau Decays in The Constrained MSSM-Seesaw Model

Vael HAJAHMAD *, Mahmoud ALBARI, Ali Ercan EKİNCİ

Erzincan Binali Yildirim University, Faculty of Arts and Sciences, Physics Department, Erzincan

Received: 20/06/2025, **Revised:** 23/07/2025, **Accepted:** 29/07/2025, **Published:** 31/12/2025

Abstract

The flavor violation of leptons may occur in specific particle interactions, a phenomenon referred to as lepton flavor violation (LFV). Within the standard model of particle physics (SM), lepton flavors are predicted to be strictly conserved. Thus, any observed violations could provide significant insights into physics beyond the standard model (BSM). This research focuses on examining LFV in tau decays within the framework of supersymmetric models (SUSY), specifically the constrained minimal supersymmetric standard model (CMSSM) which is extended by the seesaw type-I mechanism. By including right-handed neutrino fields and the seesaw mechanism, the CMSSM model offers explanations for phenomena including neutrino masses. The primary objective is to conduct a phenomenological analysis of LFV in tau decays for the following channels: $\tau^- \longrightarrow e^-e^+e^-, \tau^- \longrightarrow \mu^-\mu^+\mu^-, \tau^- \longrightarrow e^-\mu^+\mu^-, \tau^- \longrightarrow \mu^-e^+e^-, \tau^- \longrightarrow e^+\mu^-\mu^-, \tau^- \longrightarrow \mu^+e^-e^-$. We meticulously calibrated the parameters using the constraints from the current experimental bounds on neutrino and supersymmetric particle masses. We calculate the branching ratios of the LFV of tau decays, the numerical results are found to be in the order of 10^{-9}**.** The prediction of the branching ratios is found to be several orders of magnitude below the current experimental bounds.

Keywords: Lepton flavor violation, Supersymmetry, Seesaw Mechanism

Kısıtlı MSSM-Seesaw Modelinde Lepton Lezzet İhlalli Tau Bozunmaları

Öz

Leptonların lezzet ihlali, belirli parçacık etkileşimlerinde ortaya çıkabilir ve bu olaya lepton lezzet ihlali (LFV) denir. Parçacık fiziğinin standart modelinde (SM), lepton lezzetlerinin kesinlikle korunacağı öngörülmektedir. Bu nedenle, gözlemlenen herhangi bir ihlal, standart modelin ötesindeki fizik hakkında önemli bilgiler sağlayabilir (BSM). Bu araştırma, süpersimetrik modeller (SUSY) çerçevesinde, özellikle de seesaw tip-I mekanizması ile genişletilmiş kısıtlı minimal süpersimetrik standart model (CMSSM) içinde tau bozunumlarında LFV'yi incelemeye odaklanmaktadır. CMSSM modeli, sağ el nötrino alanlarını entegre eder ve seesaw mekanizması, nötrino kütleleri dahil olmak üzere çeşitli fenomenleri açıklamaktadır. Temel amaç, aşağıdaki kanallarda tau bozunumlarında LFV'nin fenomenolojik analizini yapmaktır: $\tau^- \longrightarrow e^-e^+e^-, \tau^- \longrightarrow \mu^-\mu^+\mu^-, \tau^- \longrightarrow e^-\mu^+\mu^-, \tau^- \longrightarrow \mu^-e^+e^-, \tau^- \longrightarrow e^+\mu^-\mu^-, \tau^- \longrightarrow \mu^+e^-e^-$. Nötrino ve süpersimetrik parçacık kütlelerine ilişkin mevcut deneysel sınırlamalardan elde edilen kısıtlamaları kullanarak parametreleri titizlikle kalibre ettik. Tau bozunumlarının LFV'sinin dallanma oranlarını hesapladık ve sayısal sonuçların10^{-9}. Dallanma oranlarının tahmini, mevcut deneysel sınırların birkaç mertebe altında bulunmuştur.

Anahtar Kelimeler: Lepton lezzet ihlali, Seesaw Mekanizma, Süpersimetri

Corresponding Author: whahmad@erzincan.edu.tr

Cite this Article: Erzincan University Journal of Science and Technology 2025, 18(3) 842-857. https://doi.org/10.18185/erzifbed.1723439

Introduction

The Standard Model (SM) of particle physics has been remarkably successful in describing the known elementary particles and their interactions. However, it fails to provide a mechanism for neutrino mass generation, a deficiency highlighted by the experimental confirmation of neutrino oscillations. This phenomenon implies the violation of lepton flavor in the neutral lepton sector and strongly motivates the search for physics beyond the Standard Model (BSM). One of the most well-studied frameworks that address some of the shortcomings of the SM is the Minimal Supersymmetric Standard Model (MSSM), which introduces a supersymmetric partner for each SM particle. MSSM offers attractive theoretical advantages, such as the stabilization of the Higgs mass hierarchy and the unification of gauge couplings at high energy scales. Nevertheless, it does not accommodate neutrino masses by itself. To resolve this, the MSSM can be extended by a Type-I seesaw model, in which three heavy right-handed neutrinos are introduced. This allows for the generation of small Majorana masses for left-handed neutrinos via high-scale interactions. When the universality of soft SUSY-breaking parameters is assumed at a high-energy scale, the model becomes the Constrained MSSM (CMSSM), reducing the number of free parameters and improving predictability. In such a setup, the inclusion of the seesaw mechanism induces charged lepton flavor violation via radiative corrections involving the neutrino Yukawa couplings. Among the various (LFV) observables, rare tau decays are of particular interest, especially the purely leptonic three-body decay modes, which include: $\tau^- \rightarrow e^- e^+ e^-$, $\tau^- \rightarrow \mu^- \mu^+ \mu^-$, $\tau^- \rightarrow e^- \mu^+ \mu^-$, $\tau^- \rightarrow \mu^- e^+ e^-$, $\tau^- \rightarrow e^+ \mu^- \mu^-$, $\tau^- \rightarrow \mu^+ e^- e^-$.This work presents a comprehensive phenomenological analysis of these six LFV tau decay channels within the CMSSM extended by the Type-I seesaw mechanism. The study investigates how the corresponding branching ratios are affected by key supersymmetric parameters such as the universal scalar mass m_0, gaugino mass $M_{1/2}$, trilinear coupling A_0, ratio of Higgs vacuum expectation values tanβ, and the sign of the Higgsino mass parameter μ. By exploring the parameter space, we aim to uncover distinctive features of LFV in the SUSY-seesaw framework and evaluate the model's testability in current or future experiments.

Literature Review and Experimental Constraints

Several theoretical works have established the relevance of lepton flavor violating (LFV) tau decays in the context of supersymmetric seesaw models. In particular Antusch et al. [1] and Ilakovac et al. [2] have performed direct computations of three-lepton tau decay modes such as $\tau^- \rightarrow \mu^- \mu^+ \mu^-$, $\tau^- \rightarrow e^- e^+ e^-$, $\tau^- \rightarrow e^- \mu^+ \mu^-$, $\tau^- \rightarrow \mu^- e^+ e^-$ in both Type-I and inverse seesaw models. These studies demonstrated the dependence of branching ratios on the seesaw scale, the structure of the neutrino Yukawa couplings, and SUSY-breaking parameters. Additionally, Abada et al. [3] emphasized the role of non-dipole operators, showing that decay ratios can differentiate among new physics operators. Wang et al. [4] contributed with a detailed RG-evolution formalism for Type-I seesaw models, which we incorporate in our analysis to evolve parameters from high-energy input to the electroweak scale. Building upon these foundations, our work investigates all six LFV tau decay channels under the constrained MSSM seesaw framework [5]. The present bounds and future sensitivities for these decay modes are taken

directly from the original publications of the BaBar and Belle collaborations, as summarized in the table below.

Table 1. Current Limits and Future Projections for Rare Tau LFV Decays.

LFV Process	BR Present Bound	Future Sensitivity
$\tau^- \rightarrow e^- e^+ e^-$	2.7×10^{-8} [6]	$\sim 1.0 \times 10^{-9}$ [7]
$\tau^- \rightarrow \mu^- \mu^+ \mu^-$	2.1×10^{-8} [6]	$\sim 1.0 \times 10^{-9}$ [7]
$\tau^- \rightarrow e^- \mu^+ \mu^-$	2.7×10^{-8} [6]	$\sim 1.0 \times 10^{-9}$ [7]
$\tau^- \rightarrow \mu^- e^+ e^-$	1.8×10^{-8} [6]	$\sim 1.0 \times 10^{-9}$ [7]
$\tau^- \rightarrow e^+ \mu^- \mu^-$	1.7×10^{-8} [6]	$\sim 1.0 \times 10^{-9}$ [7]
$\tau^- \rightarrow \mu^+ e^- e^-$	1.5×10^{-8} [6]	$\sim 1.0 \times 10^{-9}$ [7]

CMSSM Models and the Seesaw Mechanism

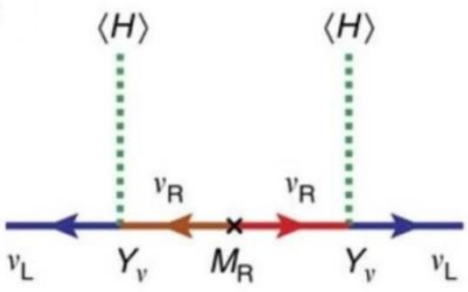

Figure 1. Canonical Seesaw Model Type-I.

The seesaw mechanism is one of the most compelling theoretical frameworks to explain the smallness of neutrino masses compared to other fermions in the Standard Model [8]. In the Type-I seesaw model, heavy right-handed neutrinos (ν_R) are introduced, which are singlets under the Standard Model gauge group and can carry large Majorana masses (M_R) [9]. These right-handed neutrinos interact with left-handed neutrinos (ν_L) via Yukawa couplings ($Y\nu$) and the vacuum expectation value of the Higgs field.

$$M\nu = -\langle H \rangle^2 \, Y\nu \, M_R^{-1} \, Y^T\nu$$

This equation, widely used in neutrino mass generation studies, demonstrates that the light neutrino mass Mν is suppressed by the large mass scale M_R of the right-handed neutrinos. The larger the M_R, the smaller the resulting mass of the left-handed neutrino, which is the core idea of the seesaw effect [9]. The accompanying Feynman diagram, shown in Figure 1, illustrates this process: a left-handed neutrino (ν_L) couples to a heavy right-handed neutrino (ν_R) via Yukawa interaction and Higgs exchange, then returns to Feynman diagram, showing ν_L propagating to itself via an intermediate heavy ν_R exchange through Higgs interactions ($\langle H \rangle$), resulting in an effective light neutrino mass as shown in Figure 1.

Main Characteristics and SUSY-Breaking Mechanism in the CMSSM

The super partners of the known Standard Model particles make up the MSSM's minimum particle content, which is preserved by the CMSSM. These super partners are introduced to preserve the symmetry of fermions and bosons [10, 11]**.** Supersymmetry breaks at high energies, often at the scale of the Grand Unified Theory (GUT), according to the CMSSM [10]. The breaking of supersymmetry results in the introduction of soft SUSY-breaking components into the Lagrange, such as mass terms, trilinear couplings, and bilinear Higgs terms.

$$-L_{soft,\ lepton} = \sum_{i=gen} \quad m_{\tilde{L}i}^2 \tilde{L}_i^\dagger \tilde{L}_i + m_{\tilde{l}_{Ri}}^2 \tilde{l}_{Ri}^\dagger \tilde{l}_{Ri} + m_{\tilde{\nu}_{Ri}}^2 \tilde{\nu}_{Ri}^\dagger \tilde{\nu}_{Ri}$$
$$+ \sum_{i,j=gen} \quad A_{ij}^l y_{ij}^l \, \tilde{l}_{Ri} H_d \tilde{L}_j + A_{ij}^\nu y_{ij}^\nu \, \tilde{\nu}_{Ri} H_u \tilde{L}_j + h.c.$$

The terms $m_{\tilde{L}i}^2$, $m_{\tilde{l}_{Ri}}^2$ and $m_{\tilde{\nu}_{Ri}}^2$ correspond to the squared mass terms of the supersymmetric partners of the left-handed leptons, right-handed charged leptons, and right-handed neutrinos, respectively. The indices i and j denote the generation number, referring to the first, second, or third family of leptons. The quantities $T_{ij}^l = A_{ij}^l y_{ij}^l$, $T_{ij}^\nu = A_{ij}^\nu y_{ij}^\nu$: A_{ij}^l and A_{ij}^ν represent the trilinear coupling terms for the charged leptons and neutrinos, respectively. Here, A_{ij}^l and A_{ij}^ν are the trilinear scalar coupling coefficients, while y_{ij}^l and y_{ij}^ν are the respective Yukawa couplings. The abbreviation h.c. stands for Hermitian conjugate, indicating that the Hermitian conjugate of the preceding term should also be included to ensure the Lagrangian is Hermitian [13].

Similarly, the lagrangian can be constructed to describe the interactions and behaviors of both the Higgs and gaugino fields [12]. At the grand unified theory (GUT) scale, $A_l = A_d = A_u = A_\nu = A_0$ represents the common scalar trilinear coupling in the constrained MSSM (CMSSM). In the CMSSM, $m_{1/2}$ denotes the universal gaugino mass $M_1 = M_2 = M_3 = m_{1/2}$. m_0 denotes the square of the symmetry-breaking masses of both supersymmetric fermions and Higgs doublets combining to a common value: $m_{\tilde{l}_R}^2 = m_{\tilde{L}}^2 = m_{\tilde{\nu}}^2 = m_0^2\ I\ \&\ m_{\tilde{H}_u}^2 = m_{\tilde{H}_d}^2 = m_0^2$. sign(μ) denotes the sign of the MSSM's supersymmetric Higgs mass parameter. tan (β) reflects the ratio of the vacuum expectation values of the two Higgs fields in the framework of the Minimal Supersymmetric Standard Model (MSSM) [15]. Msusy is the predicted scale at which supersymmetry will be achieved, which is commonly regarded as the average mass of the

supersymmetric particles (Msusy =1000GeV) [16]. The ratio of the Higgs vacuum expectation values, tanβ, is defined at the electroweak scale, while sign(μ) simply indicates the sign of the Higgsino mass parameter and is not associated with a particular energy scale.

Renormalization Group Equations (RGEs) and Lepton Flavor Violation

Renormalization group equations (RGEs) are a set of mathematical expressions that elucidate the way couplings and parameters in a given theory evolve as the energy scale at which the theory is probed,changes and varies. The equations of reorganization incorporate the quantum aspects of particle interactions and contribute to facilitating the understanding of how the characteristics of a specific theory change as we transition from high-energy scale to low-energy scale. The significance of RGEs in the context of Supersymmetry and Lepton Flavor Violation (LFV) [17]. Supersymmetric theories, such as CMSSM models, employ RGEs to explore the evolution of supersymmetry-breaking parameters and couplings with respect to changes in energy scale. The RGEs enable the examination of the behavior of supersymmetric models at various energy scales by accounting for the impacts of particle interactions and renormalization [12]. In the supersymmetric Seesaw Type-I model, two key parameters govern the radiative effects transmitted via RGEs: the neutrino Yukawa coupling matrix ($\boldsymbol{y_\nu}$) and the right-handed neutrino mass matrix M_R [18]. These parameters play a crucial role in generating LFV through the running of soft mass parameters. Specifically, the mass matrix of the left-handed sleptons acquires an additional RGE-induced contribution that leads to flavor-violating off-diagonal entries. This contribution is given by:

$$\Delta m_{\tilde{L}}^2 = -\frac{1}{8\,\pi^2} m_0^2 \left\{ 3 + \frac{A_0^2}{m_0^2} \right\} Y_\nu^\dagger Y_\nu \; log \left(\frac{M_{GUT}}{M_R} \right)$$

This equation demonstrates how the presence of the Yukawa coupling matrix (Y_ν) leads to non-universality in the slepton soft masses, a necessary condition for observable LFV processes in the left-handed slepton sector [19]. In contrast, the mass matrix of the right-handed sleptons does not receive any analogous contribution under the leading-log approximation, and remains flavor-diagonal in this framework:

$$\Delta m_{\tilde{e}}^2 = 0$$

Furthermore, the trilinear coupling terms associated with the charged leptons also undergo RGE evolution, acquiring corrections that are proportional to both the charged lepton Yukawa couplings and the neutrino Yukawa structure. This correction is expressed as:

$$\Delta T_l^2 = \frac{-3}{8\,\pi^2} A_0 Y_l Y_\nu^\dagger Y_\nu \; log \left(\frac{M_{GUT}}{M_R} \right)$$

These trilinear contributions are typically suppressed by the smallness of the charged lepton masses, particularly in the case of linear triplet coupling terms [15, 25].

Finally, in the constrained MSSM scenario, the trilinear scalar coupling A_0 is often expressed in terms of a dimensionless constant a_0 using the relation:

$$\frac{A_0}{m_0} = const = a_0 \Longrightarrow A_0 = a_0\, m_0$$

This parametrization reduces the number of free inputs in phenomenological analyses and facilitates numerical studies of LFV observables.

Analysis and Results

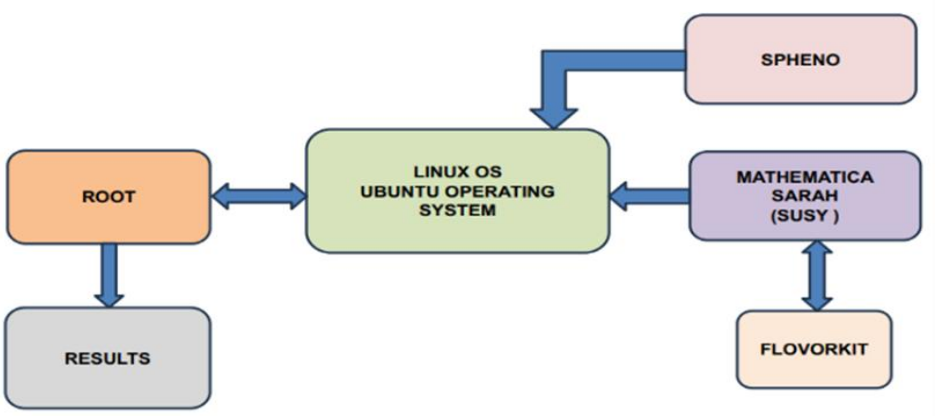

Figure 2. Workflow for SUSY Model Analysis using SPheno, SARAH, and ROOT.

In this section, the numerical results are implemented using the SARAH, SPheno and FlavorKit packages [26–29]. SARAH package is a Mathematica package for building and analyzing SUSY and non-SUSY models. It creates source code for Spheno tool. SPheno stands for S(upersymmetric) Pheno(menology). The SPheno code is written in Fortran-90 and it calculates the SUSY spectrum using low energy data and a user supplied high scale model as input like MSSM, type-I seesaw (type-II and type-III seesaw), NMSSM and other models. Furthermore, the FlavorKit package which is included in SARAH can compute a wide range of flavor observables like LFV in Z boson, Higgs and lepton decays [30-32].

Analysis of the Decay Width Γ ($\ell\alpha \to 3\ell\beta$) in Lepton Flavor Physics

$$\Gamma(\ell\alpha \to 3\ell\beta) = \frac{m_{l_\alpha}^5}{512\pi^3}\left[e^4(|K_2^L|^2 + |K_2^R|^2)\left(\frac{16}{3} log\ \frac{m_{l_\alpha}}{m_{l_\beta}} - \frac{22}{3}\right)\right.$$

$$+\frac{1}{24}(|A_{LL}^S|^2 + |A_{RR}^S|^2) + \frac{1}{12}(|A_{LR}^S|^2 + |A_{RL}^S|^2)$$

$$\left.+\frac{2}{3}\left(\left|\widehat{A_{LL}^V}\right|^2 + \left|\widehat{A_{RR}^V}\right|^2\right) + \frac{1}{3}\left(\left|\widehat{A_{LR}^V}\right|^2 + \left|\widehat{A_{RL}^V}\right|^2\right) + 6(|A_{LL}^T|^2 + |A_{RT}^T|^2)\right]$$

$$+\frac{e^2}{3}(K_2^L A_{RL}^{S*} + K_2^R A_{LR}^{S*} + \text{c.c.}) - \frac{2e^2}{3}\left(K_2^L \widehat{A_{RL}^{V*}} + K_2^R \widehat{A_{LR}^{V*}} + \text{c.c.}\right)$$
$$-\frac{4e^2}{3}\left(K_2^L \widehat{A_{RR}^{V*}} + K_2^R \widehat{A_{LL}^{V*}} + \text{c.c.}\right)$$

$$-\frac{1}{12}(A_{LL}^S A_{LL}^{T*} + A_{RR}^S A_{RR}^{T*} + \text{c.c.}) - \frac{1}{6}\left(A_{LR}^S \widehat{A_{LR}^{V*}} + A_{RL}^S \widehat{A_{RL}^{V*}} + \text{c.c.}\right)]$$

The following definition is used in the analysis: $\widehat{A_{XY}^V} = A_{XY}^V + e^2 K_1^X \quad (X, Y = L, R)$ [16].

The equation describes the decay width Γ (ℓα→3ℓβ), which represents the probability of a lepton ℓα decaying into three other leptons ℓβ. This process is relevant in the context of flavor physics, particularly in Beyond Standard Model (BSM) theories that include additional interactions.

Parameter Explanation:

- Γ(ℓα→3ℓβ): Decay width for the process where a leptonℓα decays into three leptons ℓβ.
- mℓα: Mass of the decaying lepton.
- $\boldsymbol{K_2^L, K_2^R}$: Wilson coefficients that describe the coupling of the interaction to the left-handed L or right-handed R component of the lepton.
- $\boldsymbol{A_{LL}^S, A_{RR}^S, A_{LR}^S, A_{RL}^S}$: These terms represent scalar couplings between the involved leptons.
- $\boldsymbol{\widehat{A_{LL}^V}, \widehat{A_{RR}^V}, \widehat{A_{LR}^V}, \widehat{A_{RL}^V}}$: These terms describe vector interactions, where $\boldsymbol{\widehat{A_{XY}^V}}$ s a combination of the original vector coupling $\boldsymbol{\widehat{A_{XY}^V}}$ and a term involving $\boldsymbol{K_1^X}$.
- $\boldsymbol{A_{LL}^T, A_{RT}^T}$: Tensor couplings, responsible for higher-order interactions.

Input Parameters for Numerical Analysis

The equation describes the decay rate for the transition of a lepton into three leptons of another flavor. Parameters like A_0, m_0, $m_{1/2}$, tan(β), sign(μ) influence the Wilson coefficients and therefore the couplings that mediate these decays. The processes in question are infrequent within the framework of the Standard Model and have yet to be detected through empirical observation. The final parameters in our study are: A_0, m_0, $m_{1/2}$, tan(β), sign(μ), y_ν, M_R. In the numerical analysis, models with large mixing in the neutrino Yukawa matrix y_ν are realized using the parametrization: $y_\nu = D_u U_{PMNS}^\dagger$, where y_ν is the Yukawa neutrino coupling matrix, Du is the diagonal Yukawa coupling matrix for top quarks, and UPMNS is the leptonic mixing matrix [19]. For our numerical results, we choose $m_{\nu 1} \approx$ O (10^{-3} eV). Accordingly, the heavy right-handed neutrino masses M_R are fixed as: (MR1, MR2, MR3) = (4.0×10^9 GeV, 4.0×10^9

GeV, 5.9×10¹⁴ GeV) [15]. The free parameters in the analysis are A_0, $m_{1/2}$, m_0, tan(β), while the sign of μ is taken as either positive or negative.

Analyzing the variation of BR ($\tau^- \rightarrow e^+ \mu^- \mu^-$) as a function of m_0

Figure 3 illustrates the upper limit of the branching ratio BR ($\tau^- \rightarrow e^+ \mu^- \mu^-$) as a function of m_0, for fixed values of A_0 = 300 GeV and tan(β) = 40, while varying $m_{1/2}$ in the range [160 – 460] GeV. The SUSY scale is set to M_{SUSY} = 1000 GeV. The x-axis represents m_0, and the y-axis shows the logarithmic value of the branching ratio. A shaded yellow region indicates the sensitivity range of the FCC experiment. From this figure, it is observed that the branching ratio decreases with increasing m_0 for all values of $m_{1/2}$. The highest BR values are obtained at low m_0, particularly for $m_{1/2}$ = 160 GeV. These values lie within the FCC sensitivity region up to approximately $m_0 \approx$ 600–660 GeV.

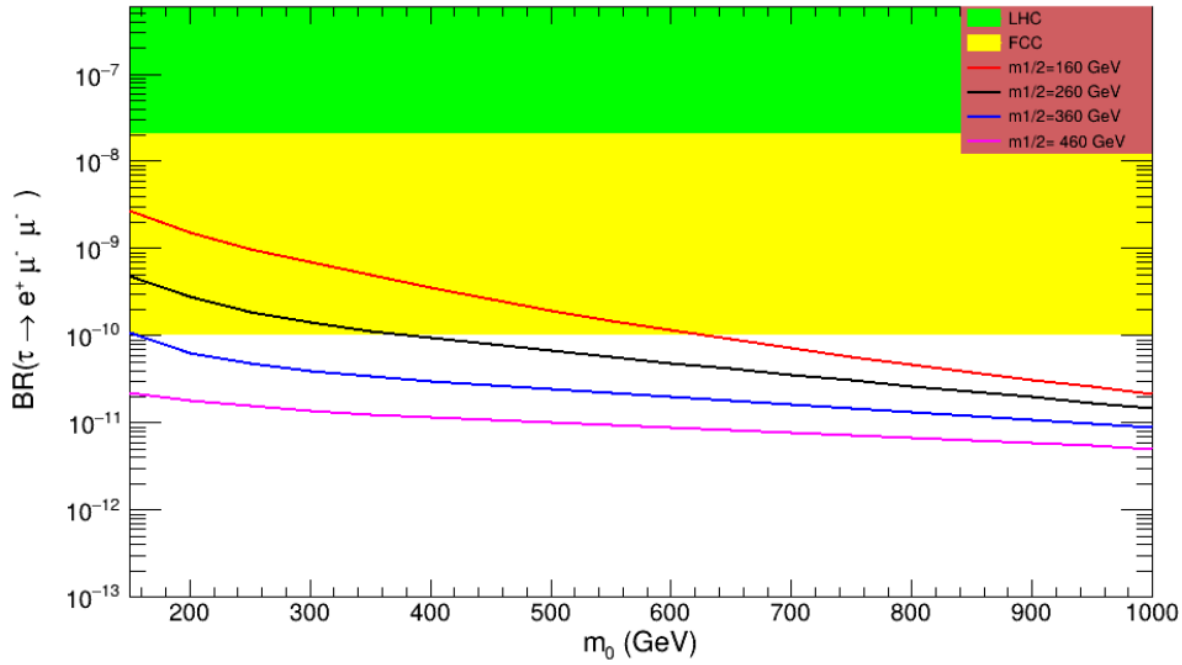

Figure 3. The upper limit of BR ($\tau^- \rightarrow e^+ \mu^- \mu^-$) as function of m_0, m_0 = [150-1000] GeV, A_0= 300 GeV, $m_{1/2}$ = [160 – 460] GeV, tan(β) = 40 and M_{SUSY} =1000 GeV.

Analyzing the variation of BR ($\tau^- \rightarrow e^- \mu^+ \mu^-$) as a function of m_0

Figure 4 presents the behavior of the branching ratio BR ($\tau^- \rightarrow e^- \mu^+ \mu^-$) as a function of the soft SUSY-breaking mass parameter m_0, under the conditions A_0 = 300 GeV and tan(β) = 40. The parameter $m_{1/2}$ varies within the range 160 to 460 GeV, while the SUSY scale is fixed at M_{SUSY} = 1000 GeV. The horizontal axis corresponds to m_0 in GeV, and the vertical axis shows the branching ratio on a logarithmic scale. Experimental sensitivity regions are highlighted: the yellow band corresponds to FCC reach, and the green region indicates the LHC exclusion limit.

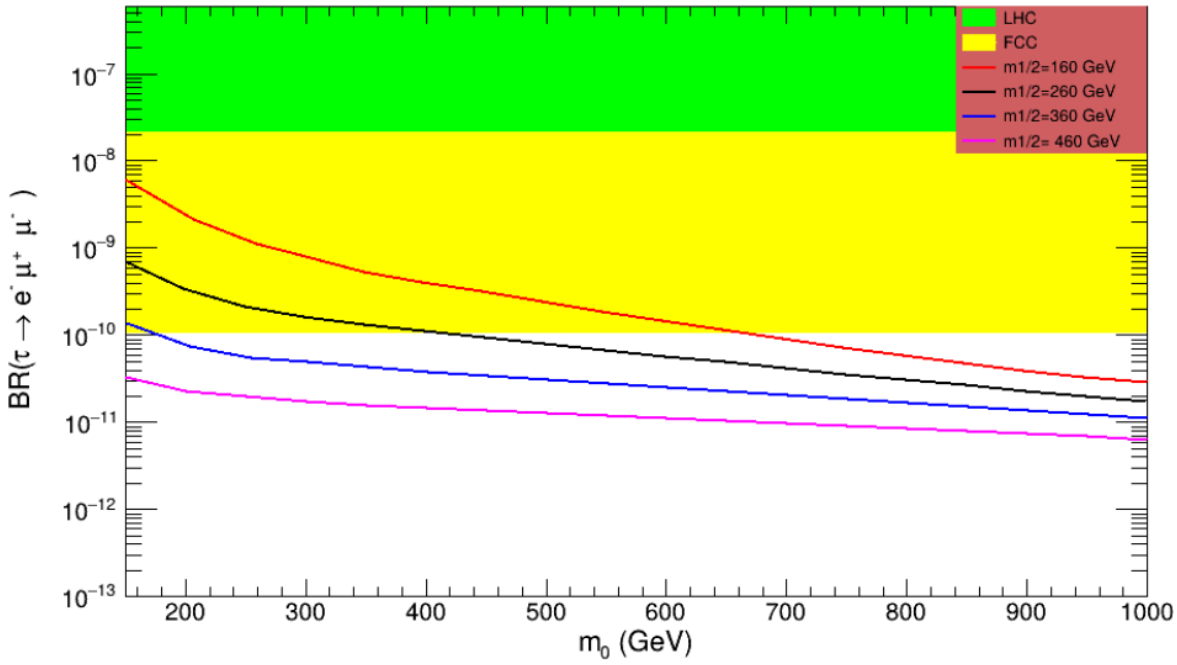

Figure 4. The upper limit of BR ($\tau^- \rightarrow e^- \mu^+ \mu^-$) as function of m_0, m_0 = [150-1000] GeV, A_0= 300 GeV, $m_{1/2}$ = [160 – 460] GeV, tan(β) = 40 and M_{SUSY} =1000 GeV.

As depicted in the figure, the branching ratio steadily declines with increasing m_0 across all values of $m_{1/2}$. The largest values of BR are obtained when $m_{1/2}$ is set to 160 GeV and m_0 is small, placing the curve well within the FCC sensitivity band up to approximately $m_0 \approx$ 600–660 GeV. This trend reinforces the conclusion that scenarios with lighter soft-breaking parameters are more likely to be observable.

Analyzing the variation of BR ($\tau^- \rightarrow \mu^+ e^- e^-$) as function of m_0

Figure 5 displays the upper limit of the branching ratio BR ($\tau^- \rightarrow \mu^+ e^- e^-$) as a function of m_0 in the range from 150 to 1000 GeV. This evaluation is conducted under the condition A_0 = 300 GeV as well as tan(β) = 40 and with four different values of $m_{1/2}$: 160 GeV (red), 260 GeV (black), 360 GeV (blue), and 460 GeV (magenta), while is M_{SUSY} = 1000 GeV. The plot highlights how the decay rate changes in response to variations in m_0 and $m_{1/2}$.

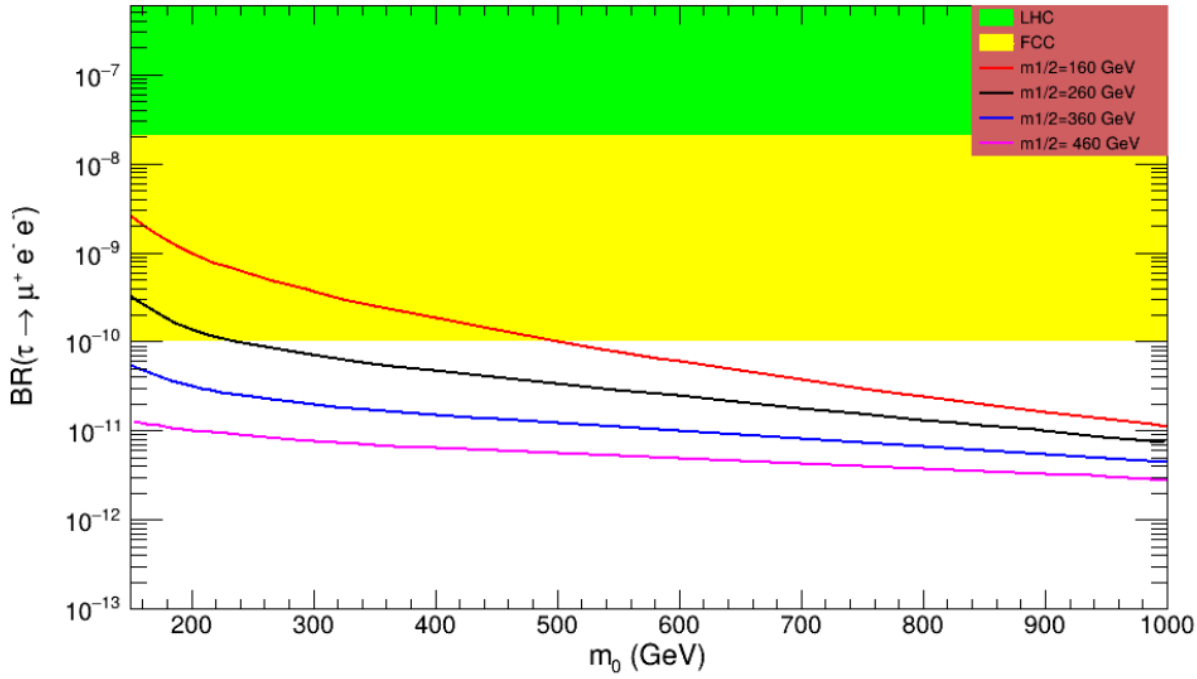

Figure 5. The upper limit of BR ($\tau^- \longrightarrow \mu^+ e^- e^-$) as a function of m_0, m_0 = [150-1000] GeV, A_0= 300 GeV, $m_{1/2}$ = [160 – 460] GeV, tan(β) = 40 and M_{SUSY} =1000 GeV.

As the value of m_0 increases, the branching ratio decreases consistently across all $m_{1/2}$ settings. This downward trend reflects the suppressive effect of larger soft-breaking mass parameters on the decay $\tau^- \longrightarrow \mu^+ e^- e^-$. Among the tested values, the most prominent decay rates are found at the lowest m_0 and smallest $m_{1/2}$, placing them within or near the sensitivity range of current and next-generation collider experiments. The dependency on m_0 and $m_{1/2}$ underscores how sensitive this process is to the supersymmetric mass configuration, while the fixed value of A_0 influences the overall scale of the branching ratio curves. Such results strengthen the case for improving experimental reach, particularly in regions of low m_0, where detection is more feasible.

Analyzing the variation of BR ($\tau^- \longrightarrow \mu^- e^+ e^-$) as function of m_0

Figure 6 presents the variation of the branching ratio (BR) for the lepton flavor-violating decay $\tau^- \longrightarrow \mu^- e^+ e^-$ as a function of the soft SUSY-breaking scalar mass parameter m_0, within the interval 150 to 1000 GeV. The analysis is carried out under the fixed conditions A_0 = 300 GeV and M_{SUSY} = 1000 GeV, while the gaugino mass parameter $m_{1/2}$ varies among the values 160 GeV, 260 GeV, 360 GeV, and 460 GeV. The colored curves in the plot correspond to these values respectively, with red representing 160 GeV, black for 260 GeV, blue for 360 GeV, and magenta for 460 GeV. As shown, the branching ratio exhibits a clear inverse correlation with m_0; as m_0 increases, BR decreases monotonically across all values of $m_{1/2}$. The highest values of BR are observed at low m_0 and low $m_{1/2}$, particularly around m_0 = 150 GeV and $m_{1/2}$ = 160 GeV.

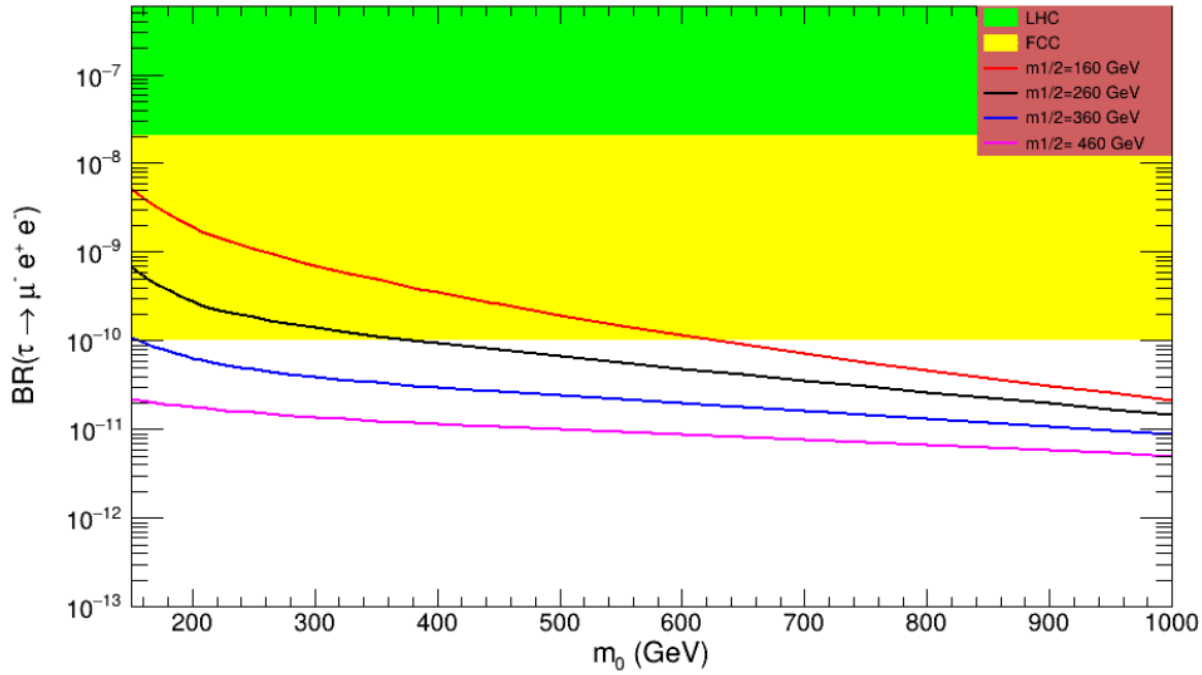

Figure 6. The upper limit of BR ($\tau^- \longrightarrow \mu^+ e^- e^+$) as a function of m_0, m_0 = [150-1000] GeV, A_0= 300 GeV, $m_{1/2}$ = [160 – 460] GeV, tan(β) = 40 and M_{SUSY} =1000 GeV.

These values place the prediction well within the projected sensitivity range of the Future Circular Collider (FCC), which is represented in yellow on the plot, while the current LHC exclusion region is indicated in green. The results highlight that scenarios with lighter soft-breaking parameters enhance the detectability of $\tau^- \longrightarrow \mu^- e^+ e^-$ decays, reinforcing the significance of future high-precision experiments in probing such rare processes.

Analyzing the variation of BR ($\tau \rightarrow 3\mu$) as a function of m_0

Figure 7 illustrates the behavior of the branching ratio (BR) for the lepton flavor-violating decay $\tau \longrightarrow 3\mu$ as a function of the soft SUSY-breaking scalar mass parameter m_0, in the range from 150 to 1000 GeV. The analysis is conducted with fixed values A_0 = 300 GeV, M_{SUSY} = 1000 GeV, and various values of $m_{1/2}$: 160, 260, 360, and 460 GeV, represented respectively by blue, black, magenta, and brown curves. The plot reveals that the branching ratio decreases progressively as m_0 increases, consistent across all values of $m_{1/2}$. The maximum branching ratio is observed for the lowest tested point: m_0 = 150 GeV and $m_{1/2}$ = 160 GeV, as shown by the blue curve. Importantly, these values place the BR well within Future Circular Collider (FCC), which is represented in yellow on the plot, while the current exclusion region of the Large Hadron Collider (LHC) is indicated in green.

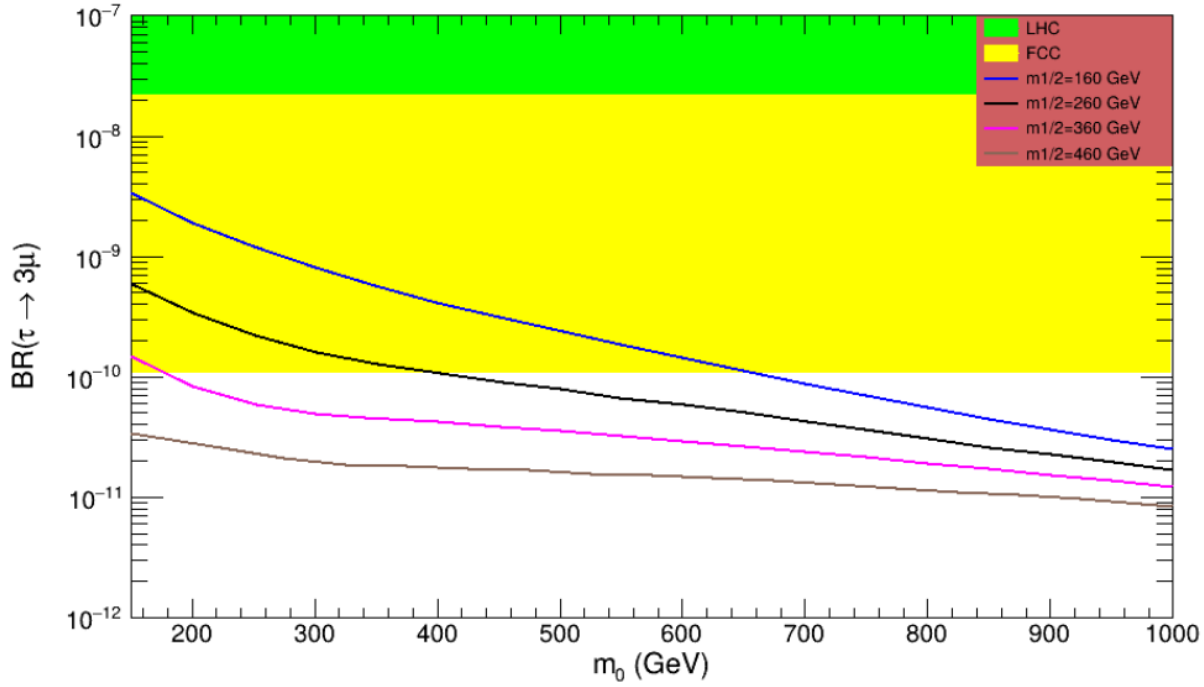

Figure 7. The upper Limit of BR ($\tau \longrightarrow 3\mu$), as function of m_0, m_0 = [150-1000] GeV, A_0= 300 GeV, $m_{1/2}$ = [160 – 460] GeV, tan(β) = 40 and M_{SUSY} =1000 GeV.

This trend highlights the importance of low-mass SUSY scenarios in enhancing the detectability of rare $\tau \longrightarrow 3\mu$ decays and motivates further investigation using current and next-generation high-precision experiments.

Analyzing the variation of BR ($\tau \rightarrow 3e$) as a function of m_0

Figure 8 illustrates the behavior of the branching ratio (BR) for the lepton flavor-violating decay $\tau \longrightarrow 3e$ as a function of the soft SUSY-breaking scalar mass parameter m_0, with a fixed trilinear coupling A_0 = 300 GeV, and SUSY scale M_{SUSY} = 1000 GeV. The gaugino mass parameter $m_{1/2}$ is varied across four values: 160 GeV, 260 GeV, 360 GeV, and 460 GeV, represented respectively by blue, black, magenta, and brown curves. As shown in the plot, the branching ratio decreases consistently with increasing m_0 for all values of $m_{1/2}$, indicating a strong inverse relationship.

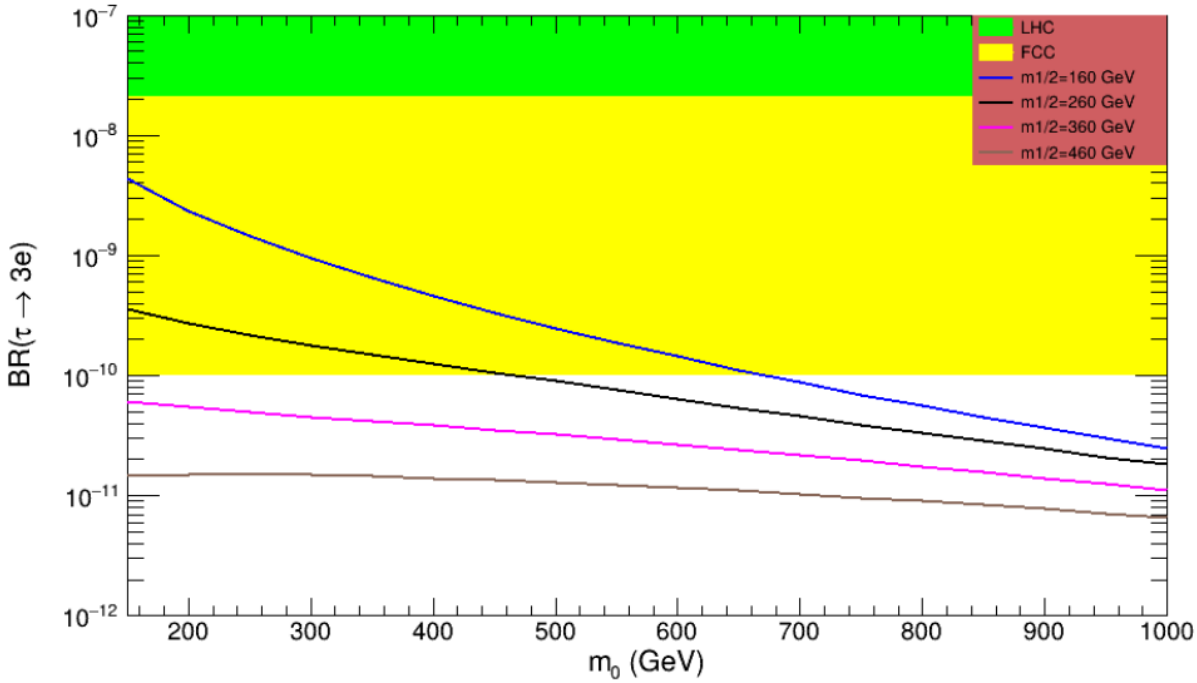

Figure 8. The upper limit of BR (τ⟶3e), as function of m_0, m_0 = [150-1000] GeV, A_0 = 300 GeV, $m_{1/2}$ = [160 – 460] GeV, tan(β) = 40 and M_{SUSY} =1000 GeV.

The highest BR is observed when $m_{1/2}$ = 160 GeV and m_0 = 150 GeV, shown by the blue curve.

Comparative Discussion and General Remarks

A comparative analysis of the six LFV tau decay channels: $\tau^- \rightarrow e^- e^+ e^-$, $\tau^- \rightarrow \mu^- \mu^+ \mu^-$, $\tau^- \rightarrow e^- \mu^+ \mu^-$, $\tau^- \rightarrow \mu^- e^+ e^-$, $\tau^- \rightarrow e^+ \mu^- \mu^-$, and $\tau^- \rightarrow \mu^+ e^- e^-$ reveals remarkably similar behavior across all modes with respect to the SUSY-breaking parameters. Each channel shows a decreasing trend in branching ratio as the soft mass parameters m_0 and $m_{1/2}$ increase.

Table 2. Summary of LFV Tau Decay Channels

Decay Channel	BR (Predicted)	Future Sensitivity	BR Present Bound
$\tau^- \rightarrow e^- e^+ e^-$	3.2×10^{-9}	$\leq 1 \times 10^{-9}$[6]	2.7×10^{-8} [7]
$\tau^- \rightarrow \mu^- \mu^+ \mu^-$	2.1×10^{-9}	$\leq 1 \times 10^{-9}$[6]	2.1×10^{-8} [7]
$\tau^- \rightarrow e^- \mu^+ \mu^-$	4.6×10^{-9}	$\leq 1 \times 10^{-9}$[6]	2.7×10^{-8} [7]
$\tau^- \rightarrow \mu^- e^+ e^-$	4.5×10^{-9}	$\leq 1 \times 10^{-9}$[6]	1.8×10^{-8} [7]
$\tau^- \rightarrow e^+ \mu^- \mu^-$	2.8×10^{-9}	$\leq 1 \times 10^{-9}$[6]	1.7×10^{-8} [7]
$\tau^- \rightarrow \mu^+ e^- e^-$	2.2×10^{-9}	$\leq 1 \times 10^{-9}$[6]	1.5×10^{-8} [7]

While some differences in sensitivity profiles exist, all predicted branching ratios lie around the order of 10^{-9} and are predominantly influenced by combinations of m_0, $m_{1/2}$. Importantly, many of these channels fall within the projected sensitivity of future experiments such as the Future Circular Collider (FCC), particularly in regions with m_0 = 150 GeV and $m_{1/2}$ = 160 GeV. These findings, summarized in Table 2, underscore the relevance of LFV tau decays in probing supersymmetric scenarios beyond the Standard Model. Moreover, when comparing the predicted branching ratios with current experimental limits, it becomes evident that most channels are already quite close to the current experimental bounds. This proximity reinforces the experimental feasibility of detecting such processes in upcoming facilities and positions these decay modes as promising targets for constraining or validating SUSY parameter spaces.

Conclusion and Outlook

In this work, we have conducted a comprehensive investigation of six lepton flavor violating (LFV) decay modes of the tau lepton: $\tau^- \to e^- e^+ e^-$, $\tau^- \to \mu^- \mu^+ \mu^-$, $\tau^- \to e^- \mu^+ \mu^-$, $\tau^- \to \mu^- e^+ e^-$, $\tau^- \to e^+ \mu^- \mu^-$, and $\tau^- \to \mu^+ e^- e^-$, within the framework of the constrained MSSM-seesaw (CMSSM + Type-I) model. In our numerical analysis, we fixed the trilinear coupling at A_0 = 300 GeV and scanned the scalar soft-breaking mass m_0 over the range [150–1000] GeV, and the gaugino mass parameter $m_{1/2}$ over the range [160–460] GeV. These parameter settings were selected to cover a wide region of phenomenologically viable SUSY scenarios. Through this detailed scan, we find that all channels show a similar sensitivity to these parameters. The predicted branching ratios are typically of the order of 10^{-9}. Notably, several channels fall within the sensitivity range of future experiments such as the Future Circular Collider (FCC), especially when m_0 = 150 GeV and $m_{1/2}$ = 160 GeV. These results indicate that LFV tau decays can offer valuable insight into supersymmetric models beyond the Standard Model.

Future Work

Our findings highlight significant advancements in the detection and measurement of rare tau decay processes. Compared to existing experimental limits, our results show considerable improvements, with several instances surpassing these benchmarks. Future projections suggest that upcoming experiments could achieve even higher sensitivities. These measurements are crucial for testing the Standard Model of particle physics and exploring new physics. Rare tau decays offer a sensitive probe for detecting new particles or interactions beyond the Standard Model. Enhanced sensitivity in these measurements could lead to groundbreaking discoveries in particle physics. Our study demonstrates substantial progress in understanding rare tau decay processes. Advanced future experiments with higher sensitivity will not only deepen our comprehension but also pave the way for uncovering new physics beyond the Standard Model.

Ethics in Publishing

There are no ethical issues regarding the publication of this study

ACKNOWLEDGMENTS

The authors thank the administration of scientific research at Erzincan Binali Yildirim University/Türkiye.

References

1. **Antusch S, Arganda E, Herrero MJ, Teixeira AM.** "LFV in tau and muon decays within SUSY seesaw." *arXiv:hep-ph/0610439*. Published online 2006.

2. **Ilakovac A, Pilaftsis A.** "Flavour-violating charged lepton decays in seesaw-type models." *Nucl Phys B.* 1995;437(3):491–526. *arXiv:hep-ph/9403398*.

3. **Abada A, Alonso R, De Romeri V, Vicente A.** "Enhancing lepton flavour violation in the supersymmetric inverse seesaw beyond the dipole contribution." *JHEP.* 2014;2014(4):1–36. *arXiv:1401.4266*.

4. **Wang W, Zhang Z, Wang Z.** "RG evolution and lepton flavor violation in Type-I seesaw." *Eur Phys J C.* 2015;75(12):597. *arXiv:1509.05388*.

5. **Hisano J, Moroi T, Tobe K, Yamaguchi M.** Lepton-flavor violation via right-handed neutrino Yukawa couplings in supersymmetric standard model. *Phys Rev D.* 1996;53(5):2442–2459.

6. **Hayasaka K, Inami K, Miyazaki Y.** Search for lepton flavor violating Tau decays into three leptons with 719 million produced $Tau^{+}Tau^{-}$ pairs. Phys Lett B. 2010; 687:139–143.

7. **Aushev T, Bartel W, Bondar A, Brodzicka J, Browder TE, Chang P, et al.** Physics at super B factory. arXiv [Preprint]. arXiv:1002.5012.

8. **Arganda E, Herrero MJ.** "Lepton flavour violation in constrained MSSM-seesaw models". arXiv08100160. Published online 2008.

9. **J. Masias, N. Cerna-Velazco, J. Jones-Perez, and W. Porod**. "Resolving a challenging supersymmetric low-scale seesaw scenario at the ILC", Phys. Rev. D 103, 115028 (2021)

10. **Hirsch M,Joaquim F,Vicente A**. **"**Constrained SUSY seesaws with a 125 GeV Higgs", Journal of High Energy Physics (2012) 2012(11), 10.1007/JHEP11(2012)105.

11**. I.J.R. Aitchison and A.J.G. Hey.** "Gauge Theories in Particle Physics", Volume 2 (Taylor & Francis, 2013)

12**. Jones, J.** L. "Gauge coupling unification in MSSM + 5 flavors". Physical Review D, 79(7), 075009 (2008).

13. **Goto T, Okada Y, Shindou T, Tanaka M, Watanabe R.** "Lepton flavor violation in the supersymmetric seesaw model after the LHC 8 TeV run". Phys Rev D. 2015;91(3):33007.

14. **Srednicki, Mark.** "Quantum field theory. Cambridge University Press, 2007", Chapter 22

15**. Girrbach J, Mertens S, Nierste U,** Wiesenfeldt S. "Lepton flavour violation in the MSSM". J High Energy Phys. 2010;2010(5):1-48.

16**. Berezinsky, V., and Kachelriess, M.** "Monte Carlo simulation for jet fragmentation in SUSY-QCD." CERN-TH 2000-232, IFIC/00-49. arXiv preprint hep-ph/0009053, 2000.

17. **Wang, Y., Zhang, D., & Zhou, S. (2023).** "Complete one-loop renormalization-group equations in the seesaw effective field theories". arXiv preprint arXiv:2302.08140

18**. J. F. Kamenik and M. Nemevšek.** "Lepton flavor violation in type I+ III seesaw," J. High Energy Phys., vol. 2009, no. 11, p. 23, 2009

19. **V. Brdar, A. J. Helmboldt, S. Iwamoto, and K. Schmitz.** "Type I seesaw mechanism as the common origin of neutrino mass, baryon asymmetry, and the electroweak scale," Phys. Rev. D, vol. 100, no. 7, p. 75029, 2019.

20**. G. Cvetič, C. Dib, C. S. Kim, and J. D. Kim**. Phys. Rev. D 66, 034008 – Published 13 August 2002; Erratum Phys. Rev. D 68, 059901 (2003)

21. **A. Abada, D. Das, A. Vicente, and C. Weiland.** "Enhancing lepton flavour violation in the supersymmetric inverse seesaw beyond the dipole contribution," J. High Energy Phys., vol. 2012, no. 9, pp. 1–34, 2012.

22**. K. Hayasaka, et al.** "Search for Lepton Flavor Violating τ Decays into Three Leptons with 719 million Produced τ+τ- Pairs", Phys. Lett. B687 (2010) 139.

23. **E. Arganda and M. J. Herrero**, Phys.Rev. D73 (2006), 055003, [hep-ph/0510405]

24. **Goodsell, M.D., Nickel, K. & Staub, F.**, "Two-loop Higgs mass calculations in supersymmetric models beyond the MSSM with SARAH and SPheno", Eur. Phys. J. C 75, 32 (2015).

25. **Bernigaud, J., Forster, A.K., Herrmann, B.**, et al, "Data-driven analysis of a SUSY GUT of flavour", J. High Energ. Phys. 2022, 156 (2022).

26. **Staub, F.,** Computer.Physics.Commun. **181**, 1077–1086 (2010) https://doi.org/10.1016/j.cpc.2010.01.011 arXiv:0909.2863 [hep-ph]

27. **Staub, F.,** Computer.Physics.Commun. **185**, 1773–1790 (2014) https://doi.org/10.1016/j.cpc.2014.02.018 arXiv:1309.7223 [hep-ph]

28. **Goodsell, M.D., Nickel, K., Staub, F.,** Eur. Phys. J. C **75** (2015) https://doi.org/10.1140/epjc/s10052-014-3247-y arXiv:1411.0675 [hep-ph]

29. **Bernigaud, J., Forster, A.K., Herrmann, B., King, S.F., Porod, W., Rowley, S.J.,** J. High Energ. Phys. **2022** (2022) https://doi.org/10.1007/JHEP05(2022)156 arXiv:2111.10199 [hep-ph]

30. **Porod, W., Staub, F., Vicente, A.,** Eur. Phys. J. C **74** (2014) https://doi.org/10.1140/epjc/s10052-014-2992-2 arXiv:1405.1434 [hep-ph]

31. **Bi, X.-J., Dei, Y.-B., Qi, X.-Y.,** Phys. Rev. D **63**, 096008 (2001) https://doi.org/10.1103/PhysRevD.63.096008, arXiv:hep-ph/0010270 [hep-ph]

32. **Navas, S.,** (Particle Data Group), Phys. Rev. D **110**, 030001 (2024) https://doi.org/10.1103/PhysRevD.110.030001